Chemistry and the hydrogenases

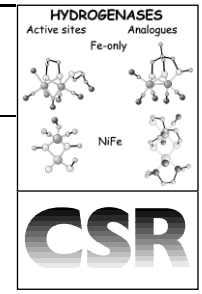

David J. Evans and Christopher J. Pickett

Department of Biological Chemistry, John Innes Centre, Norwich Research Park, Colney, Norwich NR4 7UH. E-mail: dave.evans@bbsrc.ac.uk. E-mail: chris.pickett@bbsrc.ac.uk

Received 23rd December 2002
First published as an Advance Article on the web 21st May 2003

The reversible reduction protons to dihydrogen:

$$2H^+ + 2e \rightleftharpoons H_2$$

is deceptively the simplest of reactions but one that requires multistep catalysis to proceed at practical rates. How the metal–sulfur clusters of the hydrogenases catalyse this interconversion is currently the subject of extensive structural, spectroscopic and mechanistic studies of the enzymes, of synthetic assemblies and of *in silico* models. This is driven both by curiosity and by the view that an understanding of the underlying chemistry may inform the design of new electrocatalytic systems for hydrogen production or uptake, pertinent to energy transduction technology in an 'Hydrogen Economy'. Can chemists design materials that replace the expensive platinum metal catalysts of fuel cells with metal–sulfur cluster assemblies utilising abundant Ni, Fe and S as in the natural systems? Here we review the state of the art.

Introduction

To perform difficult chemistry at ambient temperatures and pressure nature utilises extraordinary metallo-sulfur clusters (Figure 1). For example: the active site of molybdenum nitrogenase, an enzyme that fixes atmospheric nitrogen as ammonia, is an $MoFe_7XS_9$ assembly where X is an interstial C, N or O atom held in a trigonal prismatic array of six of the iron atoms;[1] at the heart of carbon monoxide dehydrogenase, an enzyme which catalyses the interconversion of carbon dioxide and carbon monoxide, is a unique $\{NiFe_4S_5\}$ assembly.[2,3] The active sites of the hydrogenases also possess biologically bizarre features—not least cyanide and carbon monoxide ligation. Normally associated with inhibition and poisoning, CO and CN^- are essential structural ligands with implicit electronic or functional roles in the biocatalysis.

We first provide a summary of the biological role of the hydrogenases, the structures of their active sites and how they are thought to function. With this backdrop we then focus on structural, mechanistic and catalytic chemistry of synthetic assemblies.

The biological rôle of the hydrogenases

Hydrogenases, first discovered by Stephenson and Stickland in 1931 in colon bacteria,[4] are found in diverse organisms. These include methanogenic, acetogenic, nitrate and sulfate reducing bacteria; anaerobic archaea, rhizobia, protozoa, fungi; and anaerobically adapted algae. It has been estimated that some 200 million tonnes of hydrogen are produced *and* consumed in anoxic habitats.[5] Anaerobic producer organisms generate dihydrogen fermentively by oxidation of carbohydrates, lipids *etc.*, the proton being the terminal electron-acceptor. A range of consumer organisms, such as methanogenic archaea, then utilise this hydrogen as an energy source – a 'microecological hydrogen economy'. Sensing hydrogen as an energy source is thus important in regulating genes that encode for uptake hydrogenases and certain bacteria, such as *Ralstonia eutropha*, have evolved 'receptor' hydrogenases and signalling pathways that respond to the intracellular hydrogen status.[6] Some bacteria internally recycle dihydrogen. Dihydrogen is always generated as a co-product of dinitrogen reduction by the nitrogenase system, the nitrogen fixing bacterium *Azotobacter vinelandii* has an uptake hydrogenase which allows recovery of some of the energy expended in the fixation process as do rhizobial

Dave Evans graduated from the University of Wales, Cardiff, at the age of twenty, with a first class honours, BSc in chemistry (1980) and subsequently a PhD in organometallic chemistry (1983). After postdoctoral research in the chemistry departments of the Universities of Arizona (USA) and York (UK) he joined the AFRC Unit of Nitrogen Fixation, Sussex (1986). The laboratory was relocated to the John Innes Centre, Norwich (1995) where he is a Project Leader in the Department of Biological Chemistry.

On completing his PhD in electrochemistry under Derek Pletcher at Southampton in 1975, Chris joined Joseph Chatt's Unit of Nitrogen Fixation at Sussex and began to learn a little more bioinorganic chemistry. Now, under the labs' current guise, he is Associate Head of Department. In 1993 he was awarded the RSC Medal for Chemistry and Electrochemistry of the Transition Metals and in 2000 an Honorary Professorship at UEA. Great friends, colleagues and students especially Jean Talarmin at Brest, Steve Best at Melbourne and Barry Smith locally have (arguably) preserved his sanity.

 DOI: 10.1039/b201317g

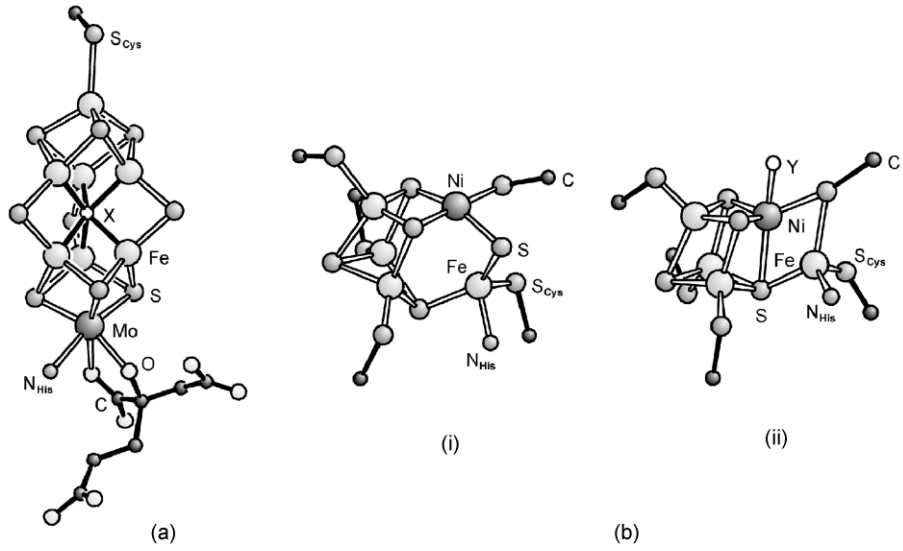

Fig. 1 The active site structures, determined by X-ray crystallography, of (a) the iron–molybdenum cofactor of molybdenum nitrogenase, X is C, N or O, and (b) nickel-containing carbon monoxide dehydrogenase: (i) reduced form; (ii) pre-incubated with carbon monoxide, Y represents an unidentified group probably non-substrate CO.

symbiotes such as *Bradyrhizobium japonicum* which nodulates legumes.[7]

There are three classes of hydrogenase: nickel–iron hydrogenases which are generally involved in hydrogen uptake; iron-only hydrogenases which are bi-directional but usually associated with hydrogen production; and transition metal free hydrogenases discovered by Thauer and coworkers,[5] but which have so far only been recognised in methanogenic archaea. We confine our discussion to the transition metal containing hydrogenases.

Structure and function of NiFe and Fe-only hydrogenases

The enzymes

In both NiFe and Fe-only hydrogenases the active sites are deeply buried within the protein matrix. For example, the NiFe-centre in the hydrogenase from *Desulfovibrio gigas* is about 30 Å from the molecular surface. Transport of H^+/H_2 to or from the active sites almost certainly takes place through specific channels in the protein matrix and the sites are 'wired' to the surface for electron exchange with their partner redox proteins by a conduit of iron–sulfur clusters, as illustrated for the Fe-only hydrogenase from *D. desulfuricans*, Figure 2.[8] What is particularly important is that the hydrogenases can sustain extremely high turnover rates and this begins to place their catalyses in the technological frame as alternatives to precious metals in hydrogen production/fuel cell applications. For example, Armstrong and co-workers have recently shown that an electrode with an adsorbed film of NiFe hydrogenase from *Allochromatium vinosum* can sustain diffusion controlled oxidation of hydrogen at the same current density as that for the platinum covered electrode. Although a higher overpotential is necessary to drive the enzyme system at diffusion limit rates it may be possible to tailor the enzymes or design free-standing active sites that operate near the thermodynamic optimum (*e.g.* near −420 mV at pH 7).[9]

The catalytic site of NiFe hydrogenase

The NiFe hydrogenase from *D. gigas*, as aerobically isolated in the inactive form, has been characterised by X-ray crystallography (Figure 3a).[10] This shows that the active site, where dihydrogen is converted to protons and electrons, is a dinuclear thiolate-bridged nickel–iron complex (Figure 3b). The nickel atom is coordinated by four cysteinate-sulfur atoms, two of which bridge to the iron atom. In the aerobically isolated crystals there is an additional bridging feature, probably oxo or hydroxo, which is not present in the active form of the enzyme (Figure 3c). The other ligands to iron, as shown by crystallography and spectroscopy,[10] are diatomic cyanide and carbon monoxide. Several other, similar, structures of NiFe hydrogenase have since been reported.[11]

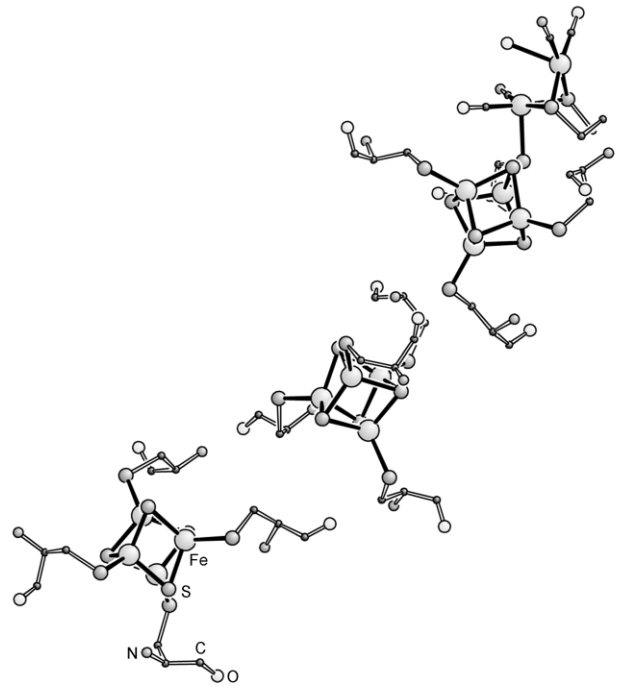

Fig. 2 The iron–sulfur clusters of the Fe-only hydrogenase from *D. desulfuricans*.

Extensive experimental studies and theoretical calculations have led to several proposals for the mechanism of NiFe hydrogenase action.[12,13,14] A simplified mechanism is shown in Scheme 1. Current thinking is that the iron atom remains low-spin Fe^{II} throughout the enzymatic cycle and that the nickel oxidation state varies. The CO and CN ligands at iron undoubtedly impose the low-spin state at this metal. Discussion

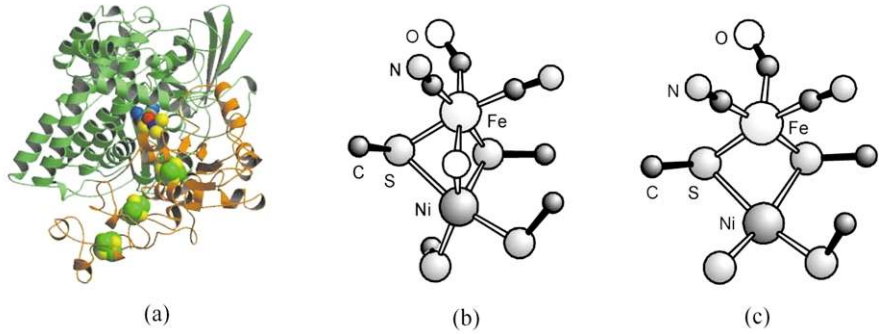

Fig. 3 The structure of (a) NiFe hydrogenase from *D. gigas*, (b) the active site of the aerobically isolated, inactive form of the enzyme and (c) the proposed "active" active site.

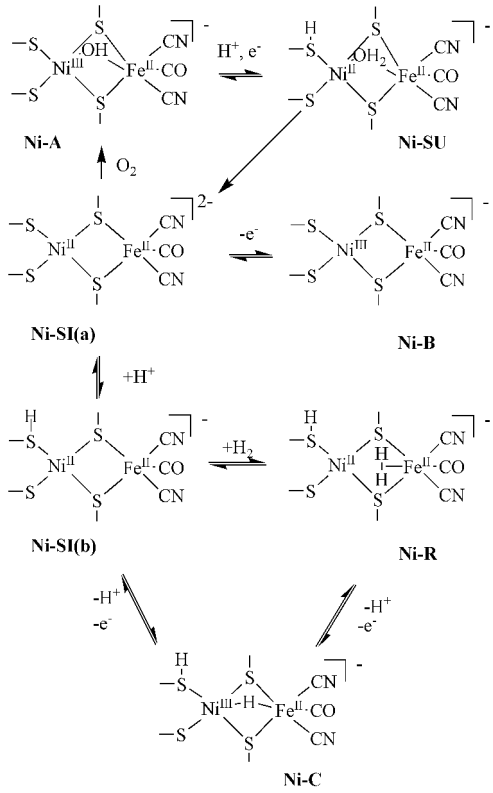

Scheme 1 Proposed enzymatic mechanism for NiFe hydrogenase

of the enzymatic cycle has generated its own shorthand for various states of the enzyme and this annotation is used in Scheme 1. Ni–A, equivalent to the aerobically isolated, inactive form, and Ni–SU can be activated to Ni–SI(a) only by incubation with dihydrogen over a period of several hours. Ni–B is a "ready form" of the enzyme as it is rapidly activated by reduction to Ni–SI(a). It has been suggested that protonation of a terminal cysteine ligand to nickel in Ni–SI(a) generates Ni–SI(b), the starting point for the enzymatic cycle, this then reacts with dihydrogen to produce Ni–R where dihydrogen is suggested to be bound side-on at iron. Single electron oxidation of Ni–R is then thought to liberate a proton to give Ni–C in which there is a hydride bridge between the iron and nickel. A further single electron oxidation releases this hydride as a proton regenerating Ni–SI(b) and completing the cycle. It has been proposed that Ni–SU, Ni–SI and Ni–R have Ni^{II} whereas Ni–A, Ni–B and Ni–C have Ni^{III}. Ni^{I} may also be involved during the enzymatic cycle. Earlier interpretation of spectroscopic results had led to the suggestion that Ni^{II} was low-spin in the forms Ni–SU, Ni–SI and Ni–R. However, more recent measurements and theoretical calculations imply that the Ni^{II} should be considered high-spin.[14] Theoretical calculations show that the optimized geometry about high-spin Ni^{II}, pseudo-tetrahedral, in the Ni–SI(a) and Ni–R forms is much closer to those observed in the crystal structures of the enzyme than if calculations assume low-spin Ni^{II}.

The catalytic site of Fe-only hydrogenase

X-ray crystallographic structures of Fe-only hydrogenases from *D. desulfuricans* and *Clostridium pasteurianum*,[8,15] together with spectroscopic data on Fe-only hydrogenase from *D. vulgaris*,[16] show that the H-cluster, the active site at which protons are reduced to dihydrogen, is a conventional $\{Fe_4S_4\}$-cluster linked by a bridging cysteinyl sulfur to an "organometallic" $\{Fe_2S_3\}$ sub-site (Figure 4). At the sub-site a terminal

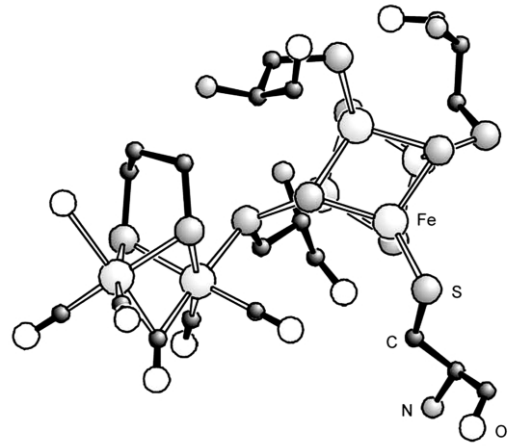

Fig. 4 A composite structure of the H-centre of Fe-only hydrogenase constructed from the crystal structures of Fe-only hydrogenase isolated from *D. desulfuricans* and *C. pasteurianum* and FTIR data from *D. vulgaris*.

carbon monoxide, a bridging carbon monoxide and a cyanide ligand are bound at each iron atom which also share two bridging sulfur ligands of a 1,3-propanedithiolate or possibly the related di(thiomethyl)amine unit. The Fe atom distal to the $\{Fe_4S_4\}$-cluster has a coordinated water molecule (or vacancy) in the resting paramagnetic oxidised state of the enzyme, $\{H_{ox}\}$. This site is occupied by carbon monoxide in the CO inhibited form of the enzyme $\{H_{ox}(CO)\}$ and is therefore thought to be where hydride/dihydrogen is bound during turnover.

The oxidation states of the two Fe centres in the sub-site of the enzyme has been the subject of some debate.[17,18] In the epr active $\{H_{ox}\}$-state, the proximal iron atom is almost certainly diamagnetic Fe^{II} because only weak magnetic coupling of the paramagnetic {4Fe4S} cluster to the sub-site is observed.[19] Thus the spin density in the sub-site resides on the distal Fe atom. The question is whether this metal atom has a formal oxidation state of Fe^{III} or is in a biologically unprecedented Fe^{I} state. It has been argued on the basis of Mössbauer data that the distal iron is in a conventional Fe^{III} state, however Fe^{I} could not

be excluded. On the other hand, FTIR ^{13}CO labelling studies of the enzyme by De Lacey and co-workers strongly support an Fe^{I} oxidation state for the distal iron centre in $\{H_{ox}(CO)\}$ because the uncoupled ν(CO) stretch at this centre is *lower* in energy than that for the CO bound at the proximal Fe^{II} site.[20] Clear support for an $\{Fe^{I}_{distal}–Fe^{II}\}$ arrangement comes from studies of synthetic {2Fe3S}-systems[21] and from DFT calculations[22] as discussed below.

Whether the bridging dithiolate at the sub-site is 1,3-propanedithiolate or a di(thiomethyl)amine unit is still an open question. Re-analysis of the first structures of Fe-only hydrogenases marginally favoured the latter ligand and led to the speculation that the amine group could function in proton delivery to the active site, as shown by Scheme 2.[23] However, a recent higher resolution structure of Fe-only hydrogenase from *Clostridium pasteurianum* has not allowed discrimination between NH and CH_2 at the '2-position' of the bridging dithiolate.†

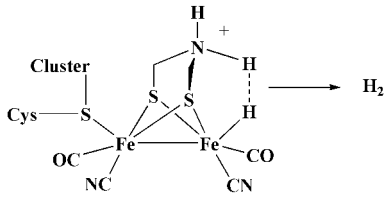

Scheme 2 Possible rôle of di(thiomethyl)amine unit.

Synthetic assemblies and chemical precedents

The mechanisms outlined in Schemes 1 and 2 are clearly based upon much conjecture. For example, for both NiFe and Fe-only hydrogenases and indeed all biological systems in which a rôle for hydrides has been invoked, there is no direct spectroscopic data establishing the presence of metal–hydride (M–H) bonds nor direct evidence for dihydrogen intermediates. This is not too surprising since strong M–H bonds would be an anathema to fast catalysis as would stable enzymic metal–H_2 intermediates. The indirect biological evidence for hydride and dihydrogen intermediates rests largely with the formation of HD during enzymic turnover under an atmosphere of D_2 and/or with the formation of HDO under this gas.[24] However, such observations do not unequivocally eliminate H/D exchange chemistry taking place at sulfur or even at CO or CN sites *via* formation of hydroxycarbenes or aminocarbenes, however unlikely this may seem.

Studies of synthetic analogues of the active sites of the hydrogenases in which for example proton, hydride or dihydrogen bonding interactions are stabilised or 'frozen-in' by tuning redox state and/or ligand environment should provide crucial insights into the enzymic hydrogen evolution/uptake chemistry. Other key questions which model studies are beginning to address are: why are two metal centres necessary for the biocatalyses; why are the biologically unusual ligands CO and CN necessary structural elements at the active sites; what is the mechanistic role of bridging/terminal CO interconversion during turnover of Fe-only hydrogenase; what are the likely metal atom redox states involved in biocatalysis; and what are the minimum structural requirements necessary for NiFe or FeFe assemblies to display hydrogenase chemistry? Beyond providing chemical precedence for putative structures, intermediates and mechanisms in the biocatalyses, synthetic analogues of the active sites provide a means of validating interpretations of the spectroscopy of the enzyme systems and to 'ground' *in silico* DFT estimates of structural and spectroscopic properties of the active sites.

† Professor John Peters, University of Utah, personal communication.

Synthetic NiFe-systems

Before the crystal structure of NiFe hydrogenase was reported it was thought that the active centre of the enzyme comprised a mononuclear or dinuclear nickel thiolate. The resultant research into the synthesis of relevant nickel coordination complexes has been reviewed elsewhere.[25] Soon after the first NiFe hydrogenase structure was published there was growing interest in the synthesis of heterodimetallic complexes with nickel and iron.[26,27] One example of such a complex came from Darensbourg's group, [{NiL-*S*}$Fe(CO)_4$] [H_2L = *N,N′*-bis(ethanethiol)-1,5-diazacyclooctane],[26] and another from the group of Pohl, [{NiL′-*S,S′*}$Fe(NO)_2$] (H_2L' = *N,N′*-diethyl-3,7-diazanonane-1,9-dithiol)[28] (Figure 5). Neither of these, unlike the active site of the enzyme, had both a bis(thiolate-bridge) between nickel and iron and CO bound to the iron atom but did have one or other of these features.

Evans and co-workers have used the anions $[Fe(NS_3)(CO)]^-$ and $[Fe(NS_3)(NO)]^-$ (NS_3 = $N(CH_2CH_2S)_3^{3-}$) as chelate ligands to nickel to prepare NiFe-complexes which have structural features with similarities to the active site of NiFe hydrogenase and some features similar to those of the active sites of the bifunctional enzyme carbon monoxide dehydrogenase/acetyl-CoA synthase. The reaction, under a CO atmosphere, of $[NEt_4][Fe(NS_3)(CO)]$ with $[NiCl_2(dppe)]$ (dppe = ethane-1,2-diphenylphosphine) gave the dinuclear complex [{$Fe(NS_3)(CO)_2$-*S,S′*}NiCl(dppe)] **1** (Figure 6).[29,30] The iron atom of complex **1** is octahedrally coordinated, with two of the thiolate ligand arms also bridging to the nickel atom. The nickel is five-coordinate in a square pyramidal pattern in which the nickel atom is displaced slightly from the base plane towards the chloride ligand in the apical site. The NS_3 ligand has the three thiolate sulfur atoms arranged meridionally about the iron and the pair of mutually *trans* thiolate arms of the ligand are essentially mirror images. The carbonyl ligands are opposite the amino nitrogen atom and one of the bridging sulfur atoms. Nickel and iron both have an oxidation state of two. Complex **1** is a good structural analogue of the proposed active site of NiFe hydrogenase (Figure 7). The core of **1** is dinuclear with nickel bound to iron by a bis(thiolate-bridge) and the iron atom binds two carbon monoxides. The Ni···Fe distance of 3.31 Å is

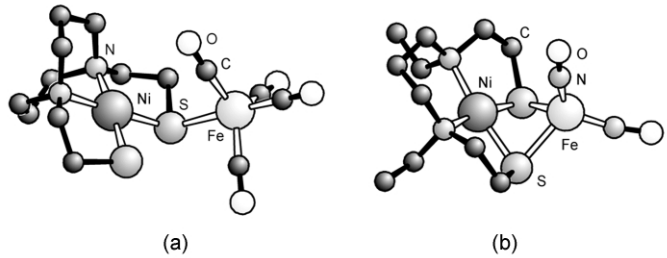

Fig. 5 The structure of (a) [{NiL-*S*}$Fe(CO)_4$] {H_2L = *N,N′*-bis(ethanethiol)-1,5-diazacyclooctane} and (b) [{NiL′-*S,S′*}$Fe(NO)_2$] {H_2L' = *N,N′*-diethyl-3,7-diazanonane-1,9-dithiol}.

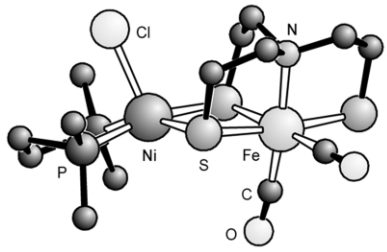

Fig. 6 A molecule of [{Fe(NS$_3$)(CO)$_2$-*S,S′*}NiCl(dppe)], phenyl groups omitted for clarity.

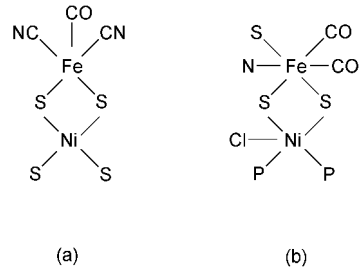

Fig. 7 A comparison of (a) the active site of NiFe hydrogenase and (b) the core of [{Fe(NS$_3$)(CO)$_2$-*S,S′*}NiCl(dppe)] **1**.

similar to that found for other thiolate-bridged nickel complexes but is longer than the Ni···Fe distance, 2.9 Å, in the as isolated, inactive NiFe hydrogenase.[10] However, theoretical calculations predict that in the active states of the enzyme the Ni···Fe distance is longer than 2.9 Å. For example, it has been calculated that the Ni···Fe distance in the Ni–SI(a) and Ni–SI(b) states, the states at which the enzyme begins the catalytic cycle, are 3.24 and 3.13 Å respectively, more similar to that found for complex **1**.[31]

When the synthesis was performed under dinitrogen or argon, rather than CO, the monocarbonyl complex [{Fe(NS$_3$)(CO)-*S,S′*}NiCl(dppe)] was formed, although always contaminated with a small amount of **1**. Attempts to introduce a cyanide ligand at iron either by direct reaction of the monocarbonyl with cyanide or by carbonyl/cyanide exchange in **1** was unsuccessful. A related complex, [{Fe(NS$_3$)(NO)-*S,S*}-NiCl(dppe)] **2** (Figure 8), can be prepared from the reaction of

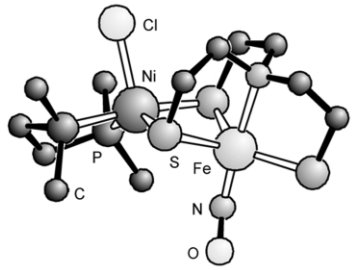

Fig. 8 A view of [{Fe(NS$_3$)(NO)-*S,S′*}NiCl(dppe)] **2**, phenyl groups omitted for clarity.

[Fe(NS$_3$)(NO)]$^-$ with [NiCl$_2$(dppe)].[30] In complex **2** the iron atom has an oxidation state of three and is trigonal bipyramidally coordinated with the nitrosyl ligand in an axial position. Similar to complex **1** two of the thiolate ligand arms also are bridging to the nickel atom. The Ni···Fe distance, 3.02 Å, is slightly shorter than that found in complex **1**.

As described earlier, the geometry about nickel is proposed to be pseudo-tetrahedral in various forms of the enzyme. Tetrahedral geometry about nickel in a thiolate environment is unusual as, in the presence of strong field donor ligands, a square planar geometry is preferred. However, a rare example of nickel in an almost regular tetrahedral thiolate environment is found in the trinuclear complex [Ni{Fe(NS$_3$)(CO)-*S,S′*}$_2$], Figure 9.[30]

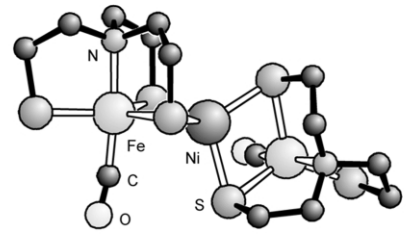

Fig. 9 Nickel in an almost regular tetrahedral thiolate environment in [Ni{Fe(NS$_3$)(CO)-*S,S′*}$_2$]

Schröder's group have prepared a dinuclear NiFe-assembly by reacting a monuclear nickel(II) thiolate precursor, [Ni(SCH$_2$CH$_2$CH$_2$S)(dppe)], with dodecacarbonyltriiron. Although full details of the crystal structure have not been published, it has been reported that in the complex [{Ni(SCH$_2$CH$_2$CH$_2$S)(dppe)-*S,S′*}Fe(CO)$_3$] **3** (Figure 10), the

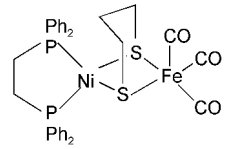

Fig. 10 A schematic representation of the structure of [{Ni(SCH$_2$CH$_2$CH$_2$S)(dppe)-*S,S′*}Fe(CO)$_3$] **3**.

Ni^{II} and Fe^0 centres are linked through the two thiolate-sulfurs of 1,3-propanedithiolate and that the metal atoms are 2.47 Å apart, a distance similar to that found by X-ray absorption spectroscopy at the active site of the enzyme from *Chromatium vinosum* on reductive activation (2.5–2.6 Å).[27] In **3** the geometry about the nickel atom is distorted tetrahedral and about iron square-based pyramidal, with two CO ligands and two thiolate-sulfurs forming the plane with the other CO in the apical position. The arrangement of ligands at iron is similar to that at the active site of the enzyme; two bridging thiolates and three diatomic ligands.

In the model complexes **1** and **3** described above, the coordination about nickel has been completed by the chelating, soft-donor, phosphine ligand, dppe. At the active site of the enzyme the ligands around nickel are all cysteinyl-thiolate. Recently, Sellmann and co-workers have prepared the first dinuclear NiFe-complex in which the nickel is coordinated only by thiolate.[32] Reaction of [Fe(CO)$_2$('S$_3$')]$_2$ ('S$_3$'$^{2-}$ = bis(2-mercaptophenyl)sulfide(2-)) with [Ni('S$_2$')(PMe$_3$)$_2$] ('S$_2$'H$_2$ = 1,2-benzenedithiol) gave [{Fe('S$_3$')(CO)(PMe$_3$)$_2$-*S,S′*}Ni('S$_2$')] **4** (Figure 11a) together with other products. In **4** four thiolate

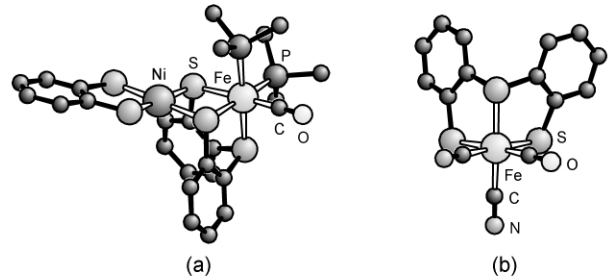

Fig. 11 The structures of (a) [{Fe('S$_3$')(CO)(PMe$_3$)$_2$-*S,S′*}Ni('S$_2$')] **4** and (b) the anion [Fe(CN)$_2$('S$_3$')(CO)]$^{2-}$.

donors in a planar geometry bind the Ni^{II} atom and the Fe^{II} is pseudo-octahedrally coordinated. The Ni···Fe distance of 3.32 Å is similar to that of complex **1**. The phosphine ligands are no

longer bound to nickel but are now on the iron atom. Sellmann's group also have reported the synthesis of the mononuclear anion $[Fe(CN)_2('S_3')(CO)]^{2-}$ (Figure 11b) which has a ligand environment about iron very similar to that found in the enzyme, with two cyanide ligands and one carbon monoxide.[33] The Fe···CN distances (1.91 and 1.93 Å) and Fe···CO distance (1.78 Å) are similar to those found, for example, within the enzyme from *D. gigas* (Fe···CN = 1.9 Å and Fe···CO = 1.7 Å).

Synthetic models of the di-iron sub-site of iron-only hydrogenase

The crystallographic characterisations of Fe-only hydrogenase[8,15] revealed the striking resemblance of the sub-site of the H-cluster to known $[Fe_2(\mu\text{-}SR)_2(CO)_6]$ (R = organic group) complexes. This type of {2Fe2S}-assembly, first discovered by Reihlen and co-workers[34] more than 70 years ago, together with the chemistry developed by Seyferth and co-workers in the 1980's,[35] opened the way for the synthesis of sub-site models. Within a very short time three groups[36,37,38] independently reported the synthesis of the dianion $[Fe_2(SCH_2CH_2CH_2S)(CO)_4(CN)_2]^{2-}$ **5** (Figure 12a). Elegant work by

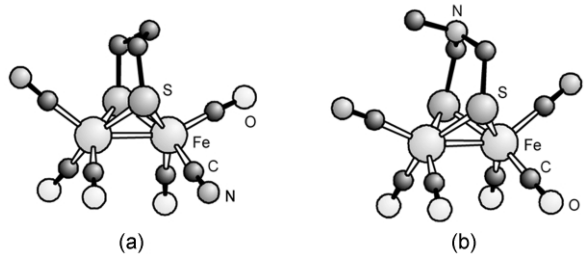

Fig. 12 Structure of dianions (a) $[Fe_2(SCH_2CH_2CH_2S)(CO)_4(CN)_2]^{2-}$ **5** and (b) $[Fe_2(SCH_2NRCH_2S)(CO)_4(CN)_2]^{2-}$ **6**.

Rauchfuss and coworkers[39] subsequently showed that the related $[Fe_2(SCH_2NRCH_2S)(CO)_4(CN)_2]^{2-}$ dianions **6** (R = H, Me) are also accessible (Figure 12b). The 'butterfly' arrangement of the dithiolate ligands in both **5** and **6** are closely similar to that in the sub-site (Figure 4) and the $\{Fe(CO)_2(CN)\}$ motifs in the complexes reasonably model the distal iron of the sub-site in the CO inhibited form of the enzyme $\{H_{ox}(CO)\}$. Two studies have addressed the mechanism of formation of **5** from the hexacarbonyl precursor. Darensbourg and co-workers have shown that the monocyanide $[Fe_2(SCH_2CH_2CH_2S)(CO)_5(CN)]^-$ can be indirectly synthesised[40] by nucleophilic attack of $[(Me_3Si)_2NLi]$ on $[Fe_2(SCH_2CH_2CH_2S)(CO)_6]$ and that it reacts with CN^- to give **5** suggesting the monocyanide is a plausible intermediate in the overall dicyanation reaction. However, Rauchfuss and coworkers[41] have proposed a dicyanation pathway, which invokes fast attack on an undetected bridging CO monocyanide intermediate because the rate of formation of **5** from the parent hexacarbonyl and CN^- is apparently *faster* than from the monocyanide. The mechanism of cyanation of {2Fe3S}-carbonyls is rather better understood as discussed below.[42]

Complexes **5** and **6** have essentially undifferentiated ligation at the two iron sites and can be viewed as possessing a {2Fe2S}- rather than the {2Fe3S}-unit as is observed within the protein. Pickett and coworkers[43] have described the synthesis of propanedithiolate ligands functionalised with an appended thioether group and showed that these allow the assembly of {2Fe3S}-carbonyls $[Fe_2\{RSCH_2C(Me)(CH_2S)_2\}(CO)_5]$ (R = Me **7** or $PhCH_2$). X-ray crystallography of **7** revealed the close similarity of the {2Fe3S}-unit in the synthetic model and that in the enzyme (Figure 13a and b).[43,44] The pentacarbonyl **7** is readily converted to a monocyanide derivative **8** in which cyanation takes place regioselectively at the Fe atom distal to the thioether ligand, Scheme 3 and Figure 13c. The reaction of **8** with further cyanide results in the formation of a moderately stable intermediate $[Fe_2\{RSCH_2C(Me)(CH_2S)_2\}(\mu\text{-}CO)(CO)_3(CN)_2]^{2-}$ **9** possessing a bridging CO, a cyanide ligand at each Fe atom, and differential ligation at the Fe atoms. These are the key structural elements of the CO inhibited sub-site of the H-cluster. **9** slowly rearranges to **10** a close {2Fe2S}- analogue of **5**, Scheme 3.

The detailed mechanism of cyanation of the carbonyl **7** has been studied by stopped-flow FTIR and UV visible spectroscopy.[42] This has: shown 'on–off' thioether ligation plays a key role in the primary substitution step; unequivocally defined the monocyanide **8** as an intermediate; and shown the bridging carbonyl species **9** is on the pathway to **10**, Scheme 3.

Whereas spectroscopy shows that the intermediate **9** possesses structural elements of the sub-site of $\{H_{ox}(CO)\}$, electronically it differs in being a diamagnetic Fe^{I}–Fe^{I} rather than a paramagnetic Fe^{I}–Fe^{II} or Fe^{III}–Fe^{II} system. Generating paramagnetic species by oxidation of precursors such as **5**, **6** or **10** has been problematic; no stable mixed valence species have been isolated. Best, Pickett and coworkers[21] have shown that a transient Fe^{I}–Fe^{II} species can be spectroscopically characterised using FTIR spectroelectrochemical and stopped-flow methods. Thus one electron oxidation of **10** generates a short-lived paramagnetic species with a bridging CO group and ν(CO) bands at wavenumbers close to those of $\{H_{ox}(CO)\}$ (Scheme 4). This strongly supports the argument of De Lacey and coworkers[20] that the $\{H_{ox}\}$ and $\{H_{ox}(CO)\}$ states of the enzyme have a mixed valence Fe^{I}–Fe^{II} unit with the spin density located on the distal Fe centre, as deduced from magnetic studies by Munck *et al.*,[18] rather than an Fe^{III}–Fe^{II} arrangement.[17] *In silico* DFT calculations on model assemblies by Cao and Hall,[22] and subsequently by Liu and Hu,[45] also conclude that $\{H_{ox}\}$ and $\{H_{ox}(CO)\}$ most likely consist of an Fe^{I}–Fe^{II} pair. Taken together the enzymic, model complex and DFT calculations all point to an unexpected rôle for Fe^{I}–Fe^{I}/Fe^{I}–Fe^{II} systems in biology. It is the π-acid ligands, CO and CN, which undoubtedly allow access to these low oxidation/spin-state levels.

It is becoming clear from FTIR studies on the enzyme system that the bridging CO of $\{H_{ox}\}$ becomes terminally bound on reduction.[20] The mechanistic implications of this may be related

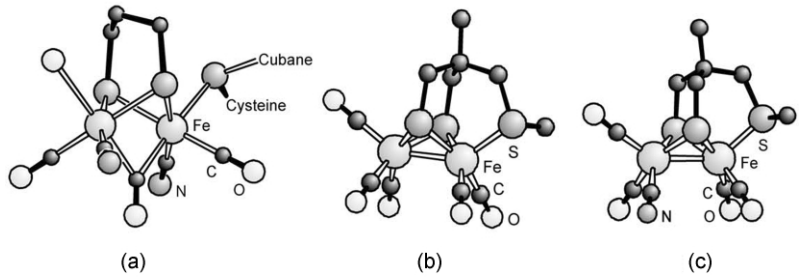

Fig. 13 A comparison of (a) the di-iron subunit of the H-cluster of Fe-only hydrogenase with (b) the molecular structure of $[Fe_2\{MeSCH_2C(Me)(CH_2S)_2\}(CO)_5]$ **7** and (c) a view of the anion $[Fe_2\{MeSCH_2C(Me)(CH_2S)_2\}(CO)_4(CN)]^-$ **8**.

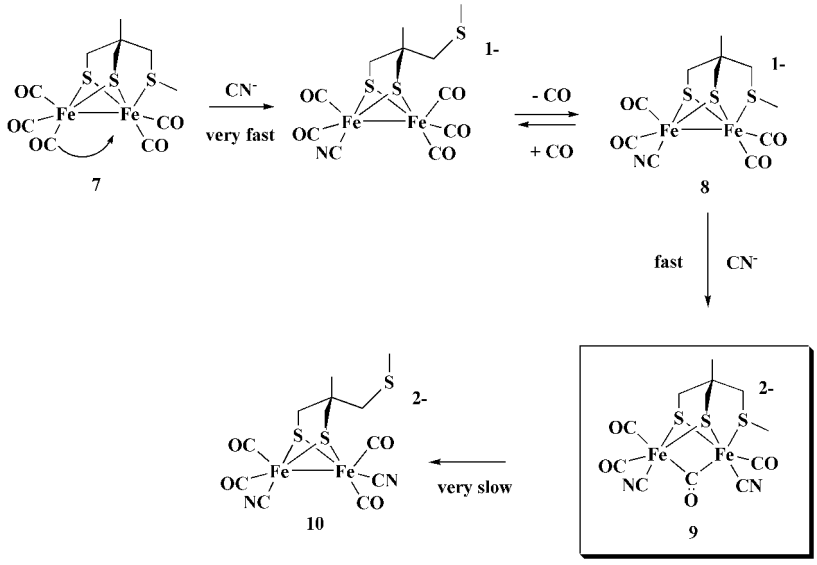

Scheme 3 Mechanism of cyanation of {2Fe3S} carbonyl.

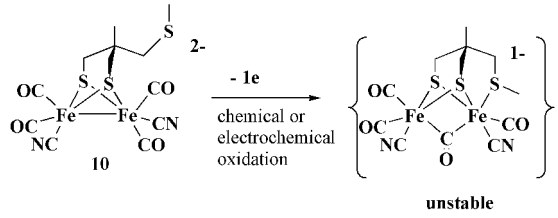

Scheme 4 Generation of Fe^{I}–Fe^{II} bridging carbonyl intermediate.

to the exposure of a proton binding site at the distal iron when CO adopts the bridging mode, with subsequent elimination of dihydrogen driven by rearrangement to a terminal CO bonding mode with concomitant metal–metal bond formation, Scheme 5. This scheme invokes formation of terminal hydride/

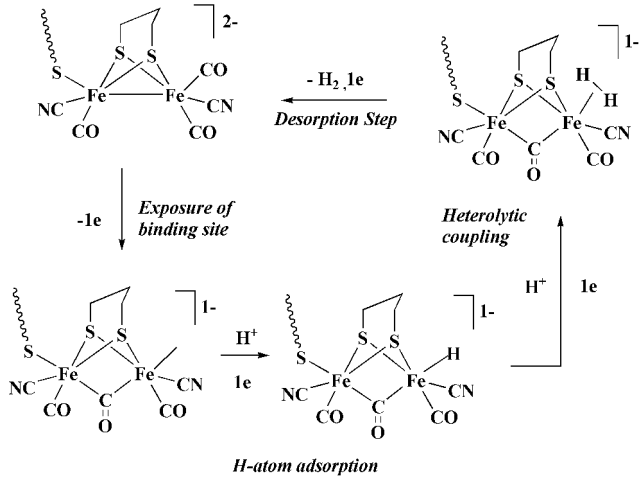

Scheme 5 Possible mechanism of proton reduction by H-centre.

dihydrogen intermediates. Such intermediates remain spectroscopically undetected in the enzymic system although indirect evidence for the involvement of hydrides in the biological system come from studies of H^+/D_2 exchange reactions.[46,47] To date no synthetic di-iron thiolate models with terminally bound hydrides have been characterised. However, tertiary phosphine di-iron dithiolate assemblies possessing a *bridging hydride* have been characterised crystallographically (Figure 14), and are shown to be capable of catalysing the H^+/D_2 exchange process.[48] Related synthetic tertiary phosphine di-iron complexes are beginning to show some evidence for

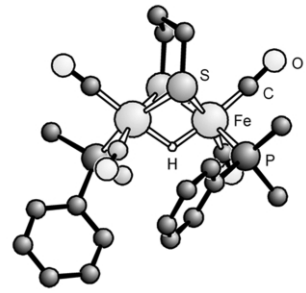

Fig. 14 The cation $[Fe_2(SCH_2CH_2CH_2S)(\mu\text{-}H)(CO)_4(PMe_2Ph)_2]^+$ with a bridging hydride.

catalysis. For example, Rauchfuss and Gloaguen[49] have provided preliminary evidence that a monocyanide derivative is capable of electrocatalytic proton reduction to dihydrogen and that the catalysis may involve both protonation at the metal–metal bond forming a bridging hydride and also protonation at the cyanide ligand, Scheme 6.

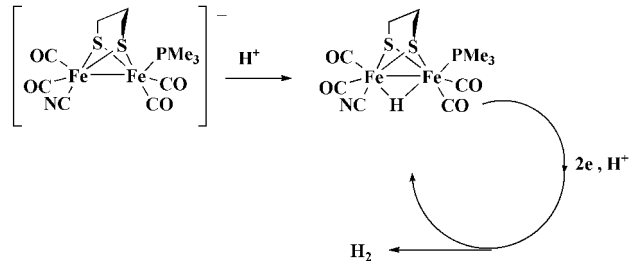

Scheme 6 Electrocatalysis of hydrogen evolution.

How the sub-site of Fe-only hydrogenase is synthesised intracellularly is not established. The source of both CO and CN^- ligands may be carbamoyl phosphate and there is some model iron chemistry that provides some precedent for this.[50] There has been some speculation on a prebiotic rôle for di-iron carbonyl thiolates. Cody *et al.*[51] have recently shown that, among other iron carbonylated species, organometallic $[Fe_2(\mu\text{-}SR)_2(CO)_6]$ derivatives can be generated from a simple chemical soup containing iron sulfide, alkanethiol and formic acid (a source of CO) possibly extant in prebiotic times. Related to this is novel chemistry described by Li and Rauchfuss[52] that utilises formaldehyde and amines in "click chemistry" to assemble azapropane dithiolate complexes, scheme 7.

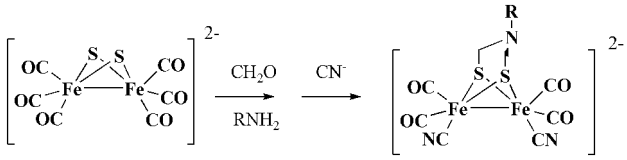

Scheme 7 "Click chemistry" for assembly of azapropanedithiolate complexes.

Concluding remarks

Redox-partner recognition sites, intra-protein electron-transfer chains, substrate/product channelling, hydrogen-bonding/dielectric modulation are necessarily imposed by the supramolecular protein architecture of the hydrogenases to achieve efficient intracellular biocatalysis. Future studies of synthetic assemblies will reveal what, if any, of this architecture is necessarily *mandatory* for designing electrocatalysts based on solid-state[53] or polymer supported Ni/Fe/S materials, further illuminate the mechanism of the natural process and offer the prospect of new biocatalysts based on artificial cofactors.

Acknowledgments

The Biotechnology and Biological Sciences Research Council is thanked for funding our research and Ms Sian Davies for assistance with preparation of the figures.

References

1 D. J. Evans, R. A. Henderson and B. E. Smith, in *Bioinorganic Catalysis*, ed. J. Reedijk and E. Bouwman, Marcel Dekker, New York, 2nd edn., 1999, ch. 7; O. Einsle, F. A. Tezcan, S. L. A. Andrade, B. Schmid, M. Yoshida, J. B. Howard and D. C. Rees, *Science*, 2002, **297**, 1696.
2 H. Dobbek, V. Svetlitchnyi, L. Gremer, R. Huber and O. Meyer, *Science*, 2001, **293**, 1209.
3 C. L. Drennan, J. Y. Heo, M. D. Sintchak, E. Schreiter and P. W. Ludden, *P. N. A. S.*, 2001, **98**, 11973.
4 M. Stephenson and L. H. Stickland, *Biochem. J.*, 1931, **25**, 205.
5 R. K. Thauer, A. R. Klein and G. C. Hartmann, *Chem. Rev.*, 1996, **96**, 3031.
6 O. Lenz, M. Bernhard, T. Buhrke, E. Schwartz and B. Friedrich, *J. Mol. Microbiol. Biotechnol.*, 2002, **4**, 255.
7 R. J. Maier and E. W. Triplett, *Crit. Rev. Plant. Sci.*, 1996, **15**, 191.
8 Y. Nicolet, C. Piras, P. LeGrand, C. E. Hatchikian and J. C. Fontecilla-Camps, *Structure*, 1997, **7**, 13.
9 A. K. Jones, E. Sillery, S. P. J. Albracht and F. A. Armstrong., *Chem. Commun.*, 2002, 866.
10 A. Volbeda, M.-H. Charon, C. Piras, E. C. Hatchikian, M. Frey and J. C. Fontecilla-Camps, *Nature*, 1995, **373**, 580; A. Volbeda, E. Garcin, C. Piras, A. L. De Lacey, V. M. Fernandez, E. C. Hatchikian, M. Frey and J. C. Fontecilla-Camps, *J. Am. Chem. Soc.*, 1996, **118**, 12989; R. P. Happe, W. Roseboom, A. Pierik, S. P. J. Albracht and K. A. Bagley, *Nature*, 1997, **385**, 126.
11 P. M. Matias, C. M. Sooares, L. M. Saraiva, R. Coelho, J. Morais, J. Le Gall and M. A. Carrondo, *J. Biol. Inorg. Chem.*, 2001, **6**, 63 and references therein.
12 A. C. Marr, D. J. E. Spencer and M. Schröder, *Coord. Chem. Rev.*, 2001, **219–221**, 1055 and references therein.
13 P. E. M. Siegbahn, M. R. A. Blomberg, M. Wirstam née Pavlov and R. H. Crabtree, *J. Biol. Inorg. Chem.*, 2001, **6**, 460 and references therein.
14 H.-J. Fan and M. B. Hall, *J. Am. Chem. Soc.*, 2002, **124**, 394 and references therein.
15 J. W. Peters, W. N. Lanzilotta, B. J. Lemon and L. C. Seefeldt, *Science*, 1998, **282**, 1853.
16 A. J. Pierik, M. Hulstein, W. R. Hagen and S. P. J. Albracht, *Eur. J. Biochem.*, 1998, **258**, 572; A. L. De Lacey, C. Stadler, C. Cavazza, E. C. Hatchikian and V. M. Fernandez, *J. Am. Chem. Soc.*, 2000, **122**, 11232; Y. Nicolet, A. L. De Lacey, X. Vernede, V. M. Fernandez, E. C. Hatchikian and J. C. Fontecilla-Camps, *J. Am. Chem. Soc.*, 2001, **123**, 1596.
17 A. S. Pereira, P. Tavares, I. Moura, J. J. G. Moura and B. H. Huynh, *J. Am. Chem. Soc.*, 2001, **123**, 2771.
18 C. V. Popescu and E. Munck, *J. Am. Chem. Soc.*, 1999, **121**, 7877.
19 K. K. Surerus, M. Chen, J. W. Vanderzwaan, F. M. Rusnak, M. Kolk, E. C. Duin, S. P. J. Albracht and E. Munck, *Biochemistry*, 1994, **33**, 4980.
20 A. L. De Lacey, C. Stadler, C. Cavazza, E. C. Hatchikian and V. M. Fernandez, *J. Am. Chem. Soc.*, 2000, **122**, 11232.
21 M. Razavet, S. J. Borg, S. J. George, S. P. Best, S. A. Fairhurst and C. J. Pickett, *Chem. Commun.*, 2002, 700.
22 Z. X. Cao and M. B. Hall, *J. Am. Chem. Soc.*, 2001, **123**, 3734.
23 Y. Nicolet, B. J. Lemon, J. C. Fontecilla-Camps and J. W. Peters, *Trends Biochem. Sci.*, 2000, **25**, 138.
24 M. W. Adams, *Biochim. et Biophys. Acta*, 1990, **1020**, 115.
25 J. C. Fontecilla-Camps, *J. Biol. Inorg. Chem.*, 1996, **1**, 91.
26 M. Y. Darensbourg, E. J. Lyon and J. J. Smee, *Coord. Chem. Rev.*, 2000, **206–207**, 533 and references therein.
27 A. C. Marr, D. J. E. Spencer and M. Schröder, *Coord. Chem. Rev.*, 2001, **219–221**, 1055 and references therein.
28 F. Osterloh, W. Saak, D. Hasse and S. Pohl, *Chem. Commun.*, 1997, 979.
29 S. C. Davies, D. J. Evans, D. L. Hughes, S. Longhurst and J. R. Sanders, *Chem. Commun.*, 1999, 1935.
30 M. C. Smith, J. E. Barclay, S. P. Cramer, S. C. Davies, W.-W. Gu, D. L. Hughes, S. Longhurst and D. J. Evans, *J. Chem. Soc., Dalton Trans.*, 2002, 2641.
31 S. Li and M. B. Hall, *Inorg. Chem.*, 2001, **40**, 18.
32 D. Sellmann, F. Geipel, F. Lauderbach and F. W. Heinemann, *Angew. Chem. Int. Ed.*, 2002, **41**, 632.
33 D. Sellmann, F. Geipel and F. W. Heinemann, *Chem. Eur. J.*, 2002, **8**, 958.
34 H. Reihlen, A. Gruhl and G. Hessling, *Liebigs Ann. Chem.*, 1929, **472**, 268.
35 D. Seyferth, G. B. Womack, C. M. Archer and J. C. Dewan, *Organometallics*, 1989, **8**, 430.
36 E. J. Lyon, I. P. Georgakaki, J. H. Reibenspies and M. Y. Darensbourg, *Angew. Chem., Int. Ed.*, 1999, **38**, 3178.
37 M. Schmidt, S. M. Contakes and T. B. Rauchfuss, *J. Am. Chem. Soc.*, 1999, **121**, 9736.
38 A. Le Cloirec, S. P. Best, S. Borg, S. C. Davies, D. J. Evans, D. L. Hughes and C. J. Pickett, *Chem. Commun.*, 1999, 2285.
39 D. Lawrence, H. X. Li, T. B. Rauchfuss, M. Benard and M. M. Rohmer, *Angew. Chem., Int. Ed.*, 2001, **40**, 1768.
40 E. J. Lyon, I. P. Georgakaki, J. H. Reibenspies and M. Y. Darensbourg, *J. Am. Chem. Soc.*, 2001, **123**, 3268.
41 F. Gloaguen, J. D. Lawrence, M. Schmidt, S. R. Wilson and T. B. Rauchfuss, *J. Am. Chem. Soc.*, 2001, **123**, 12518.
42 S. J. George, Z. Cui, M. Razavet and C. J. Pickett, *Chem. Eur. J.*, 2002, **8**, 4037.
43 M. Razavet, S. C. Davies, D. L. Hughes and C. J. Pickett, *Chem. Commun.*, 2001, 847.
44 M. Razavet, S. C. Davies, D. L. Hughes, J. E. Barclay, D. J. Evans, S. A. Fairhurst, X. Liu and C. J. Pickett, *Dalton Trans.*, 2003, 586.
45 Z. P. Liu and P. Hu, *J. Am. Chem. Soc.*, 2002, **124**, 5175.
46 X. Zhao, I. P. Georgakaki, M. L. Miller, J. C. Yarbrough and M. Y. Darensbourg, *J. Am. Chem. Soc.*, 2001, **123**, 9710.
47 J. P. Collman, P. S. Wagenknect, R. T. Hembre and N. S. Lewis, *J. Am. Chem. Soc.*, 1990, **112**, 1294.
48 X. Zhao, I. P. Georgakaki, M. L. Miller, R. Mejia-Rodriguez, C. Y. Chiang and M. Y. Darensbourg, *Inorg. Chem.*, 2002, **41**, 3917.
49 F. Gloaguen, J. D. Lawrence and T. B. Rauchfuss, *J. Am. Chem. Soc.*, 2001, **123**, 9476.
50 S. Reissmann, E. Hochleitner, H. Wang, A. Paschos, F. Lottspeich, R. S. Glass and A. Bock, *Science*, 2003, **299**, 1067.
51 G. D. Cody, N. Z. Boctor, T. R. Filley, R. M. Hazen, J. H. Scott, A. Sharma and H. S. Yoder, *Science*, 2000, **289**, 1337.
52 H. X. Li and T. B. Rauchfuss, *J. Am. Chem. Soc.*, 2002, **124**, 726.
53 C. J. Pickett, S. K. Ibrahim and D. L. Hughes, *Faraday Discuss.*, 2000, 235.